Published in final edited form as:
ACS Nano. 2009 April 28; 3(4): 1004–1010. doi:10.1021/nn900113x.

Label-Free DNA Sensor Based on Surface Charge Modulated Ionic Conductance

Xian Wang and **Sergei Smirnov***
Department of Chemistry and Biochemistry, New Mexico State University, Las Cruces, NM 88003

Abstract

The surface charge effect in controlling ionic conductance through nanoporous alumina membrane is investigated for its application in a convenient detection method of unlabeled DNA. To this goal, surface modification with mixtures of neutral silanes and morpholinos (neutral analogs of DNA) was optimized to yield a strong effect on ionic conductance change upon DNA binding, which can exceed an order of magnitude. The effect can be employed in fabrication of inexpensive DNA sensors.

Keywords

label-free sensor; ionic conductance; nanopores; surface charge effect; morpholino; DNA

INTRODUCTION

Applications of nanotechnology are particularly versatile when it comes to chemical and biochemical sensors. Bioaffinity interactions such as DNA-DNA and antigen-antibody are typically employed for identification of the presence of a particular DNA sequence in a sample, for detection and identification of microbial and viral species. The mechanism of detecting such an interaction with untagged biochemical analytes can vary broadly and utilize the change of mass, volume, charge, optical or other properties of the analytes. In this article we demonstrate that high charge of DNA oligomers can be employed in detecting its binding to the surface of nanopores by measuring ionic conductance through the pores. The technique can be conveniently extended to simultaneous measure of numerous DNA analytes.

Because of a large surface/volume ratio in nanoporous materials, the ionic conductance through the pores is greatly affected by the ions' interaction with the walls. This interaction can manifest itself through different mechanisms, most commonly via the 'volume exclusion' and the 'surface charge' mechanisms. Previously we have demonstrated the utilization of the volume exclusion mechanism for DNA detecting.[1–4] In this mechanism, small diameter pores get 'cloaked' as a result of binding targeted DNA onto single stranded DNA (ss-DNA) covalently attached to the walls. The result is detected by a drop in ionic flux through the pores. The observed effect was strongly dependent on the pore diameter: almost nonexistent with 200 nm pores and reaching in excess of 50 % in 20 nm or smaller pores.

The surface charge effect can be observed in pores of a larger diameter but, opposite to the volume exclusion mechanism, it requires low ionic strengths. When the bulk concentration of

snsm@nmsu.edu.

Supporting Information contains the concentration dependence of solution conductance, FTIR spectra of modified membranes, the representative Nyiquist and Bode plots, electrode resistance for different thicknesses of deposited gold. It is available free of charge via the Internet at http://pubs.acs.org.

electrolyte is low, surface charge on the walls dictates the concentration of ions inside the nanochannel and causes the ionic conductance to become independent of the bulk concentration [4–6]. To fulfill electroneutrality, the nanochannel is filled predominantly with the ions having an opposite charge to that of the wall surface. If an analyte such as DNA binds to the wall, it changes the surface charge and thus the ionic concentration and conductance through the nanochannel. It should be noted that, unlike the volume exclusion regime, binding of a charged analyte alter the conductance even if the overall cross section of the nanopore is unchanged.

There have been several reports suggesting that the surface charge effect can be employed as a sensing mechanism. For example, Karnik *et al.* [7] demonstrated that nanochannel modified with biotin had significantly increased ionic conductance upon binding of (charged) streptavidin. Since DNA is a highly charged molecule, the surface charge effect can be employed for DNA sensing. Jagerszki *et al.* [8] also had shown that flux of anions through a gold nanopore array modified with uncharged peptide nucleic acid (PNA) decreased upon hybridization with complementary DNA.

As we have shown [6], even when the radius of a nanochannel, a, is larger than the Debye length, r_D, defined by the ions concentration, C_{bulk}, (monovalent in this case):

$$\frac{1}{r_D}=\left[\frac{2e^2C_{\text{bulk}}}{\varepsilon_o\,\varepsilon k_B T}\right]^{1/2}. \tag{1}$$

the ions of the same charge as that of the walls are appreciably expelled from the nanochannel and the electrical current through the nanochannel is primarily carried by the ions of the opposite charge. From the electroneutrality requirement, the difference between the concentrations of oppositely charged monovalent ions of the electrolyte, ΔC, is defined by the surface charge density, σ, and the nanochannel radius, a:

$$\Delta C=\frac{2\sigma}{\text{ea}}=\frac{2N_s}{a} \tag{2}$$

It is convenient in some cases to express the charge density via the surface density of monovalent charges, $\sigma = eN_s$. Alternatively, the value ΔC itself can be used for describing the changes in the surface charge density for the pores of a given radius.

If the positive and negative ions of the electrolyte have the same diffusion constant, D, (which is very close in the case of KCl) and it is presumed to be unaltered inside the small diameter nanochannel, the ionic current through a single cylindrical nanochannel of length L under applied voltage V can be expressed as [6]:

$$I_{\text{channel}}=\frac{e^2\pi a^2}{k_B T}\frac{D\sqrt{\Delta C^2+4C_{\text{bulk}}^2}V}{L} \tag{3}$$

A membrane of the cross section area A, consisted of an array of multiple nanochannels in parallel thus making its porosity (a fraction of the cross section that is empty) equal α, would have the resistance:

$$Z_{\mathrm{mem}}=\frac{k_B T}{e^2 \alpha D \sqrt{\Delta C^2+4C_{\mathrm{bulk}}^2}}\frac{L}{A} \quad (4)$$

which is almost identical to that of the unhindered solution of the same dimensions only for $C_{bulk} \gg \Delta C$. In the opposite limit, when the concentration disparity, $\Delta C \gg C_{bulk}$, is greater, Z_{mem} becomes less than that of Z_{sol} and independent of C_{bulk}. The difference in these resistances, according to Eq.(4), can be quite significant and can be utilized with appropriately designed ligands placed inside the nanochannels. One has to realize though that when applied to detecting DNA, the ionic resistance of the membrane drops upon binding of highly charged DNA. Thus, it is desirable to have the electrodes as close as possible to the pores so that the electrolyte resistance outside the pores has minimal effect. Also, because of a low electrolyte concentration necessary for this detection scheme, nonpolarizable electrodes, such as AgCl, are not applicable and faradeic currents would be difficult to control as well. The best configuration then employs AC mode of measurement with noble electrodes such as gold that have large double layer capacitance and are directly deposited on the opposite sides of the membrane.

RESULTS AND DISSCUSIONS

Figure 2A shows the frequency dependence of the absolute impedance, $|Z_{mem}|$, (Bode plot) for an unmodified membrane with different concentrations of electrolyte. The equivalent circuit for this setup and its relation to the membrane geometry is shown in Scheme 1. The ionic resistance of the pores, R_p, in parallel with the pores' capacitance, C_p, is connected in series with the double layer capacitance, C_{dl}, of the electrodes and the electrical resistance of the electrodes, R_{el}. Placing the electrodes directly at the membrane eliminates the contribution to the resistance from solution outside the pores. This is an important feature because the surface charge effect reveals at low ionic concentrations when even small gaps between the electrodes and the pores can have comparable to the pore resistance. The chosen electrode geometry circumvents this undesired effect and leaves only the electronic resistance of the gold electrodes, which is still noticeable because of the small thickness and narrow reams of the resulting electrode mesh (see Figure 1). At high frequencies and high electrolyte concentrations, the membrane capacitance, C_p, is barely recognizable in the Bode plots (one can identify it at low electrolyte concentrations as a dip at high frequencies). The impedance of the double layer capacitance, C_{dl}, arises as a low frequency impedance rise inversely proportional to frequency. Its value has contributions from both, the Helmholtz layer, C_H, and the diffusive layer, C_{dif}:

$$\frac{1}{C_{\mathrm{dl}}}=\frac{1}{C_H}+\frac{1}{C_{\mathrm{dif}}} \quad (5)$$

The latter cause the concentration dependence ($C_{dif} \sim C_{bulk}^{1/2}$) which is visible in Figure 2. The membrane pore resistance responsible for the frequency independent part of $|Z_{mem}|$ in Figure 2, has a close to linear dependence on the electrolyte concentration. Figure 1C presents it as a function of the free solution impedance, $|Z_{sol}|$. The saturation at low $|Z_{sol}|$ (high electrolyte concentration, C_{bulk}) is due to the electrode resistance discussed above, which is on the order of 20 Ω. Variation of $|Z_{mem}|$ at low C_{bulk} (high $|Z_{sol}|$) is due to the above introduced surface charge effect and is the basis of DNA sensing proposed in this paper.

Figure 2B illustrates that Bode plots for the membrane modified with covalently bound to its surface single stranded DNA oligos (21-mers) have lower resistances at low electrolyte concentrations, which is the result of a higher surface charge brought about by DNA. The effect is clearly visible in Figure 2C, where $|Z_{mem}|$ is plotted versus $|Z_{sol}|$ for membranes with and without DNA. Since the conductivity of solution deviates from a linear dependence at low salt concentrations due to conductivity of dissociated water and dissolved carbonic acid, presenting data this way accounts for the deviation. For that reason, it is better to use not very low electrolyte concentrations, where deviation of the conductance from a linear dependence is not as severe and KCl ions are the prevailing conducting species. The concentration of 10 μM KCl is suitable for that. [10]

In this example covalently attached to the surface DNA shows a significant drop of the membrane resistance suitable for employing the effect for DNA sensing. In constructing such a DNA sensor, *i.e.*, identifying the presence of a target single stranded DNA (ss-DNA) in solution, one has to appreciate the imposed requirements of the detection method. Neutral analogs of DNA, such as PNA and morpholino, are more appropriate. Because of the neutral charge, morholoino analog of polynucleic acid is a perfect ligand to capture target ss-DNA: not only does it contribute zero charge to the surface but its hybridization with complementary DNA is practically independent of the salt concentration. The latter property is particularly useful and favors the choice of morpholino rather than attempting to achieve overall surface neutrality by matching the mixture of DNA and amines. We have tried employing another neutral analog of DNA – peptide nucleic acid (PNA) but were not successful in obtaining measurable density of its immobilization on the membrane surface.[10]

As a demonstration of applicability for this technique, we chose the sequences that can be used for identification of genetic mutation responsible for cystic fibrosis. Cystic fibrosis transmembrane conductance regulator (CFTR) is a protein responsible for transport of chloride ions across the membranes of cells in the lungs, liver, pancreas, digestive tract, reproductive tract, and skin. Genetic mutations observed in about 70% of patients [11–13] with cystic fibrosis (CF) result from deletion of three base pairs in CFTR's nucleotide sequence. This deletion causes loss of the amino acid phenylalanine located at position 508 in the protein; therefore, this mutation is referred to as ΔF508 or F508. CFTR protein with the ΔF508 mutation is incorrectly folded and prevents it from reaching the cell membrane. People who are homozygous for this mutation tend to have the most severe symptoms of cystic fibrosis due to critical loss of chloride ion transport which accounts for more than 90% of the clinical cases. [14]. The sodium and chloride ion imbalance creates a thick, sticky mucus layer that cannot be removed by cilia and traps bacteria, resulting in chronic infections. Because of a dramatic mutation, the difference in melting temperatures is significant, especially with morpholino. The correct CFTR sequence near the mutation site, ATC AT**C TT**T GGT GTT has a melting temperature, T_m, even with the complementary surface bound 15-mer 'ligand' DNA, AAC ACC AAA GAT GAT, of around $T_m \sim 45°C$. The mutant DNA of the same length (with truncated CTT), ATC ATT GGT GTT TCC, has $T_m < 25°C$. The difference is even more dramatic with morpholino/DNA pairs.

As Figure 3 illustrates, the membrane modified with aminosilane and subsequently activated by gluteraldehyde (Figure 3A) does not have its resistance significantly altered after immobilization of aminated morpholino (Figure 3B), as expected for this neutral nucleic acid analog. Hybridization with the complementary target ss-DNA, on the other hand, drops the resistance two fold. Since the mutant DNA does not hybridize readily, the resistance in this case was not significantly affected.

It is clear that at low ionic strengths (high $|Z_{sol}|$) the membrane resistance, presented as the impedance at 10 kHz, $|Z_{mem}|$, is lower than that of the unrestrained solution not only for the

membrane after hybridization with ss-DNA but, to a lower extent, for the membrane before DNA binding as well (see Figure 3D). The effective surface charge densities, measured as the ΔC values (see Eq.(2)), are $\Delta C = 9.5\times10^{-4}$ M and 4.8×10^{-4} M, for the two cases respectively. Similar effect is seen in Figure 2C, where the membrane without DNA also demonstrates departure from linear concentration dependence and the surface charge densities are characterized by $\Delta C = 1.2\times10^{-4}$ M and 8×10^{-4} M before and after DNA binding, respectively. The reason for that is a nonzero surface charge in both cases. Alumina surface has PZC (point of zero charge) exceeding pH > 8.5 and thus is positively charged at neutral pH.[15,16] Residual alumina hydroxyls, as well as amino groups from the surface modification, render the surface positively charged. [17] We observed that even if the surface is modified by ester silane, which in the perfect scenario of a monolayer formation is supposed to render the surface neutral, the surface charge does not totally disappear and retains residual charge about 25% of the original value, as judged by the value and sign of the streaming potential. The streaming potential arises from electrolyte moving in the pore under the pressure gradient and gains the value proportional to the surface charge density if the velocity profile of the liquid is the same. Upon amination with only APTS the streaming potential increases slightly because of similar charge densities of hydroxyl groups on alumina and attached amino groups. When the surface amines are activated by gluteraldehyde, the streaming potential also does not change because the resulting Schiff base is still charged.[17] Upon DNA attachment, on the other hand, the amount of positive charge decreases and its sign can change if significant portion of the activated groups are utilized for DNA binding. The density of immobilized aminated DNA is much less than the density of the surface amines. Previously we [1,18] saw that the maximum density of bound ss-DNA (15-mer) did not exceed $10^{13}/cm^2$. Thus, the charge of fully aminated surface (with the surface density on the order of $3\times10^{14}/cm^2$) decreases upon DNA binding. For that reason, the amination in Figure 3 was performed for one hour because not all amines were employed for DNA immobilization.

To better optimize the conditions for DNA sensing, we produced a series of mixed surface modifications, with different proportions of amino and ester silanes, and examined the effect of subsequent DNA binding on these surfaces. The silanization process in this case was performed to as much completion as possible by reacting the membranes with silane mixtures for 12h. Figure 4 illustrates the results of this analysis. The membrane with 100% aminated surface shows the lowest resistance, which *increases* upon DNA binding due to decreasing of the total charge, as mentioned above. Mixed amino/ester silane modifications produce fewer amines and thus fewer of them are left unreacted after DNA immobilization. Increasing the proportion of neutral ester in the modifications increases the membrane resistance before DNA binding; it also causes the effect of the resistance *drop* upon DNA binding to enhance. Eventually, at very low fractions of amine, the amount of bound ss-DNA becomes insufficient to induce the surface charge change greater than the residual charge, and the effect of resistance change upon DNA binding declines again.

According to Figure 4H, the optimal fraction of aminosilane is near 1:7 and the corresponding conductance enhancement is close to 10. The theoretical surface charge enhancement for replacing one positive charge of amine by a 15-mer DNA oligomer is 13 (15 nucleobases minus 2 Schiff bases from gluteraldehyde), which is in a remarkably good agreement with the observed factor of 10.

This optimized ratio amine:ester = 1:7 was used in construction of improved DNA sensor, where the same morpholino as in Figure 3 was immobilized on activated by gluteraldehyde silanized surface. Figure 5 depicts the resistance changes at 3 kHz in the course of hybridization/ denaturing with the complementary and mutant target DNA. When compared with the morpholino modified membrane, the resistant at first drops over seven fold after hybridization with the complementary strand but, when compared with the value after

denaturing, the effect is only four fold. Even with that incomplete recovery after denaturing, the effect is still significantly larger than that in Figure 3. Hybridization with the mutant (noncomplementary) DNA, on the other hand, barely changes the membrane resistance as compared with the value after denaturing. The overall effect of the resistance change with complementary DNA has improved compared to Figure 3 but is still less than the anticipated value of above 10 that was observed with covalent immobilization of DNA in Figure 4. The reasons for the difference have not been fully identified yet. It is likely not due to the ionic diffusion change, as we previously have observed no conductance decrease in nanopores of the same diameter after DNA hybridization [1]. These previous measurements were performed in 1.0 M KCl while the current concentration is only 10 μM but it should not make a difference. The imperfection in the signal amplitude could arise, at least in part, from: a) a lower immobilization efficiency of morpholino on the surface, as compared with similar DNA, b) its incomplete hybridization with DNA in low concentration 10 μM solution and c) ineffective denaturation procedure. We do not have any reason to suspect that the volume exclusion mechanism, that has the opposite effect on conductance, would be of any significance in pores of such relatively large diameter as used here. Previously, we proved using DNA/DNA hybridization in such membranes that the contribution of the volume exclusion mechanism was not detectable in '200 nm' pores and required 20 nm or less for it to be observed.[1,2] The supporting information illustrates it by FTIR spectra.[10] Further optimization to address these issues is required and will be the subject of future studies.

CONCLUSIONS

We have demonstrated that the surface charge effect in controlling the ionic conductance through nanoporous alumina membrane can be applied as a convenient detection method for unlabeled ss-DNA. The method was realized on the membranes with gold electrodes deposited directly on the opposite sides and the surface of nanopores modified by an optimized mixture of neutral ester silanes and morpholinos (neutral analog of DNA). Even though there is room for further optimization, it is obvious that the surface charge effect can be employed in fabrication of inexpensive electrical DNA sensors. Such a sensor would not require an electrochemical potentiostat and can be eventually employed with standard interfaces available on every computer.

EXPREIMENTAL SECTION

Surface modification

Anodized alumina membranes (AAO) from Whatman with the nominal diameter of 200 nm and 60 μm thickness were boiled in water and dried in an oven at 120°C before modification. The membranes were first modified with ethanol solution of silanes. Either sole APTS (3-amino-propyltrimethoxysilane, from Aldrich) or its mixture with ETS (2-(carbomethoxy) ethyl-trichlorosilane, from Gelest) in different proportions (APTS:ETS = 0:1, 1:20, 1:10, 1:7, 1:4, 1:2) were used. The amount of ester silane, ETS, in the mixtures was fixed at 2 w/v % and the amount of APTS was varied to achieve the desired ratio. Two options were tried: one hour of silanization by aminosilane and overnight silanization with the mixtures (including those of sole aminosilane and sole ester silane). After washing with ethanol, the membranes were baked at 120°C for 3h to ensure the completion of covalent linkage of silanes to the surface and their lateral polymerization in the monolayer. The remaining modifications (originating on the surface bound amines) were performed after deposition of gold electrodes on the membrane and after placing it inside the cell.

Cell assembly and impedance measurements

Gold electrodes (200 nm Au on 3 nm Cr underlayer) were deposited on opposite sides of the membrane using a Gatan Ion Beam Coater (681 Series) at 15° angle to the normal of the membrane. The thickness and the angle of deposition were optimized initially to minimize the electrode electrical resistance and to increase their surface area necessary for lowering the electrode impedance.[10]

The surface of each membrane was activated by overnight treatment in 5% aqueous solution of glutaraldehyde (Aldrich). After drying by nitrogen gas, the membrane was assembled into the cell, where the remaining modifications were performed. The home-made cell held the modified membrane in between the two PMMA pieces (sealed by parafilm) with matching holes for solution flow. The holes identified three independent regions for conductance measurements each with 1.5 mm diameter. The corresponding electrodes on the opposite sides of the membrane were connected to a potentiostat (700C series, from CH Instruments) for impedance measurements that were performed in the two electrode scheme under small AC voltage (≤10mV).

The Bode plots in the frequency range from 1 to 10^5 Hz were collected 90 min after the last manipulation with solution exchange. Separate measurements confirmed that to be sufficient for the signal stabilization. Various concentrations of KCl in DI water ranging from 10 μM up to 1 M were used to confirm the manifestation of the surface charge effect. The solutions were equilibrated with air to avoid variations due to dissolution of carbon dioxide, their pH was 5.5. The resistances of these solutions were also measured in a separate conductivity cell with platinum electrodes and the cell constant equal 0.3 cm^{-1}.[10] The experiments for DNA detection were typically performed at 10 μM KCl.

Immobilization of nucleic acids

Aminated nucleic acids were immobilized on the aldehyde activated membrane surfaces that are already placed inside the cell. Approximately 30 μL of ~ 100 μM solution of aminated nucleic acid (5'-aminated morpholino or 5'-aminated DNA) in DI water (Milli-Q) was injected into the cell and left overnight under a seal preventing water from evaporation. After that, the membrane was washed with 0.1 M KCl and, finally, with copious amounts of DI water.

Hybridization and denaturing procedures

Hybridization was typically performed by ~5 μM of DNA in PBS (0.1 M KCl) at room temperature for one hour. The unhybridized DNA was washed off from the membrane by copious amounts of solution to be measured in (typically 10 μM KCl). The denaturation was achieved by treatment with 9M urea, which included one hour soaking and washing with copious amounts. The treatment was finished by washing with copious amounts of the solution used in measurements.

Nucleic acids

All DNA oligomers were ordered from Integrated DNA Technologies (Coralville, IA) of HPLC purified quality and used without further purification. All sequences are given starting from 5'. The surface bound aminated DNA: /5AmMC6/AAC ACC AAA GAT AAT A. its complementary target DNA: ATC ATC TTT GGT GTT; and the mutant target DNA: ATC ATT GGT GTT TCC, represent a normal and the genetic mutation sequences for cystic fibrosis.

A neutral analog of polynucleic acid oligomer, morpholino oligo has morpholine rings instead of the deoxyribose sugar moieties connected by non-ionic phosphorodiamidate linkages replacing the anionic phosphates of DNA. Each morpholine ring attaches one of the standard DNA bases. Aminated at 5' morpholino, /5AmMC6/TTT TTT AAC ACC AAA GAT GAT,

was ordered from Gene Tools LLC (Philomath, OR). It represents a truncated 12 mer portion of the above described aminated DNA that has a six-thymine extension. Some experiments were also performed with ananologous aminated DNA 21-mer, /5AmMC6/TTT TTT AAC ACC AAA GAT GAT.

Supplementary Material

Refer to Web version on PubMed Central for supplementary material.

ACKNOWLEDGEMENTS

This work was supported in part by the National Institutes of Health (NIH S06 GM008136). The authors are also grateful to NM EPSCOR program for providing funds to purchase the potentiostat used in this study.

REFERENCES

1. Vlassiouk I, Takmakov P, Smirnov S. Sensing DNA Hybridization via Ionic Conductance through a Nanoporous Electrode. Langmuir 2005;21:4776–4778. [PubMed: 15896007]
2. Takmakov P, Vlassiouk I, Smirnov S. Hydrothermally Shrunk Alumina Nanopores and their Application to DNA Sensing. Analyst 2006;131:1248–1253. [PubMed: 17066194]
3. Smirnov S, Vlassiouk I, Rios F, Takmakov P, Gust D. Smart Nanoporous Membranes. ECS Trans 2007;3(26):23.“Bioelectronics, Biointerfaces, and Biomedical Applications 2”
4. Vlassiouk, I.; Smirnov, S. Ch. 15. In: Arben, Merkoçi, editor. Biosensing using nanomaterials. Wiley; 2009. p. 459-490.ISBN 978-0-470-18309-0
5. Stein D, Kruithof M, Dekker C. Surface-Charge-Governed Ion Transport in Nanofluidic Channels. Phys. Rev. Lett 2004;93:035901. [PubMed: 15323836](1–4)
6. Vlassiouk I, S. Smirnov S, Siwy Z. Ionic Selectivity of Single Nanochannels. Nano Letters 2008;8:1978–1985. [PubMed: 18558784]
7. Karnik R, Duan C, Castelino K, Daiguji H, Majumdar A. Rectification of Ionic Current in a Nanofluidic Diode. Nano Lett 2007;7:547–551. [PubMed: 17311461]
8. Jagerszki G, Gyurcsanyi RE, Hofler L, Pretsch E. Hybridization-Modulated Ion Fluxes through Peptide-Nucleic-Acid- Functionalized Gold Nanotubes. A New Approach to Quantitative Label-Free DNA Analysis. Nano Lett 2007;7:1609. [PubMed: 17488052]
9. Vlassiouk I. unpublished results
10. Supporting Information
11. Kerem B, Rommens JM, Buchanan JA, Markiewicz D, Cox TK, Chakravarti A, Buchwald M, Tsui LC. Identification of the Cystic Fibrosis Gene: Genetic Analysis. Science 1989;245:1073–1080. [PubMed: 2570460]
12. Riordan JR, Rommens JM, Kerem B, Alon N, Rozmahel R, Grzelczak Z, Zielenski J, Lok S, Plavsic N, Chou JL, et al. Identification of the Cystic Fibrosis Gene: Cloning and Characterization of Complementary DNA. Science 1989;245:1066–1073. [PubMed: 2475911]
13. Rommens JM, Iannuzzi MC, Kerem B, Drumm ML, Melmer G, Dean M, Rozmahel R, Cole JL, Kennedy D, Hidaka N, et al. Identification of the Cystic Fibrosis Gene: Chromosome Walking and Jumping. Science 1989;245:1059–1065. [PubMed: 2772657]
14. Chen EY, Bartlett MC, Loo TW, Clarke DM. The ΔF508 Mutation Disrupts Packing of the Transmembrane Segments of the Cystic Fibrosis Transmembrane Conductance Regulator. J. Biol. Chem 2004;279:39620–39627. [PubMed: 15272010]
15. Szczepanski V, Vlassiouk I, S. Smirnov S. Stability of Silane Modifiers on Alumina Nanoporous Membranes. J. Membr. Sci 2006;281:587–591.
16. Brown GE, Henrich VE, Casey WH, Clark DL, Eggleston C, Felmy A, Goodman DW, Gratzel M, Maciel G, McCarthy MI, et al. Metal Oxide Surfaces and Their Interactions with Aqueous Solutions and Microbial Organisms. Chem. Rev 1999;99:77–174. [PubMed: 11848981]
17. The streaming potential, $\Delta V/\Delta P=\varepsilon 0\varepsilon\zeta\eta\lambda$, arises from electrolyte moving in the pore under the pressure gradient, ΔP, and gains the value, ΔV, proportional to the surface charge density (the surface zeta

potential, ζ), where ε and η are the solvent dielectric constant and viscosity, respectively. The value decreases with increasing conductivity of the electrolyte, λ; we used 10 μM KCl. The exact correlation between ΔV and the surface charge density given in the formula depends on the velocity profile of the liquid near the channel walls. We have found that even though the streaming potential is convenient in identifying the sign of the surface charge, *e.g.*, the values are opposite for alumina and when its surface modified (negatively charged) silica, but no good correlation with the charge density was found when surfaces were modified by organic layers

18. Vlassiouk I, Krasnoslobodtsev A, Smirnov SN, Germann M. 'Direct' Detection and Separation of DNA Using Nanoporous Alumina Filters. Langmuir 2004;20:9913–9915. [PubMed: 15518473]

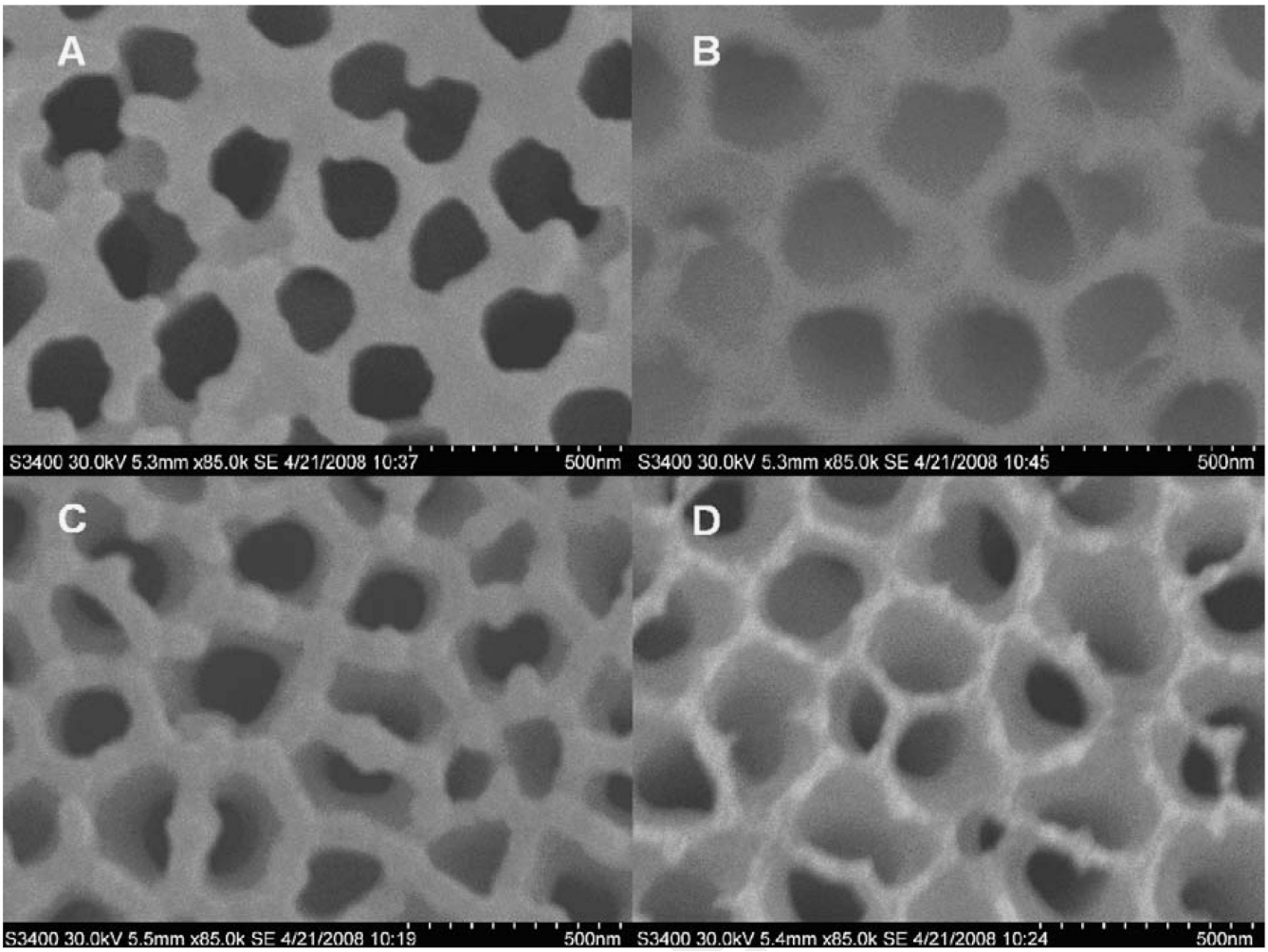

Figure 1.
SEM images of the opposite sides of an AAO membrane before (**A** and **B**) and after (**C** and **D**) deposition of 200 nm of gold.

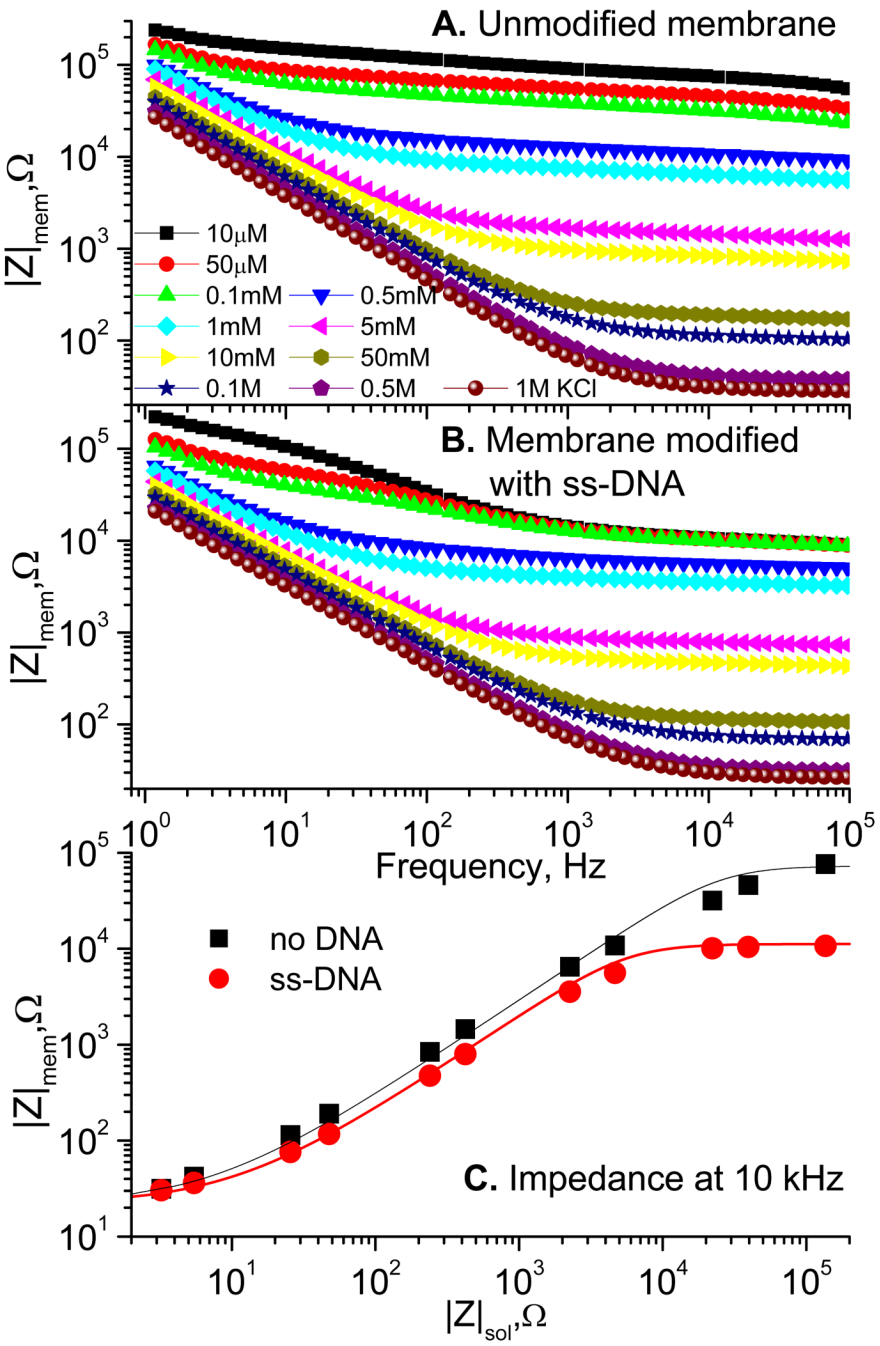

Figure 2.

Bode plots at different concentrations of KCl for an unmodified membrane (A) and a membrane on which surface ss-DNA (21-mer) was covalently immobilized via amine (for 1 hour)-gluteraldehyde chemistry (B). The Impedance at 10 kHz for membranes from A (■) and B (■) as functions of the KCl concentration measured as the impedance of free solution. The solid lines represent the best fits with R_{el} = 22 Ω and the concentration jump, $\Delta C = 1.2\times10^{-4}$ M (black), and 8×10^{-4} M (red).

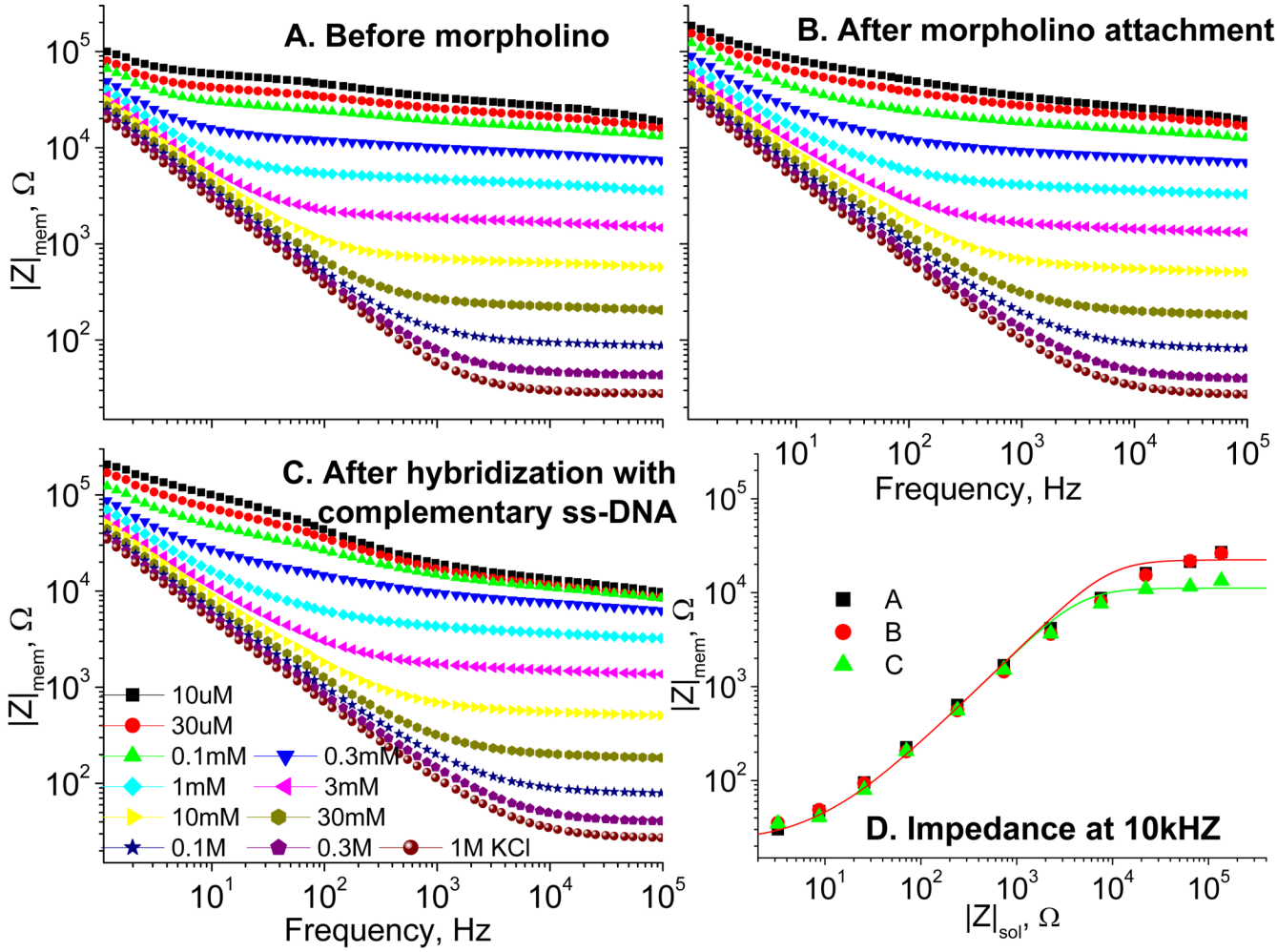

Figure 3.

Bode plots at different concentrations of KCl for the membrane modified with aminosilane (for 1 hour) and activated by gluteraldehyde (**A**); the same membrane after immobilization of the morpholino (**B**) and after hybridizing with complementary target ss-DNA 15-mer (**C**). (**D**) The Impedance at 10 kHz for membranes of **A** (■) and **B** (●) and **C** (▲) as functions of the KCl concentration measured as the impedance of free solution. The solid lines represent the best fits with R_{el} = 22 Ω and the surface charge densities, the concentration jump, ΔC = 4.8×10^{-4} M (red), and 9.5×10^{-4} M (green).

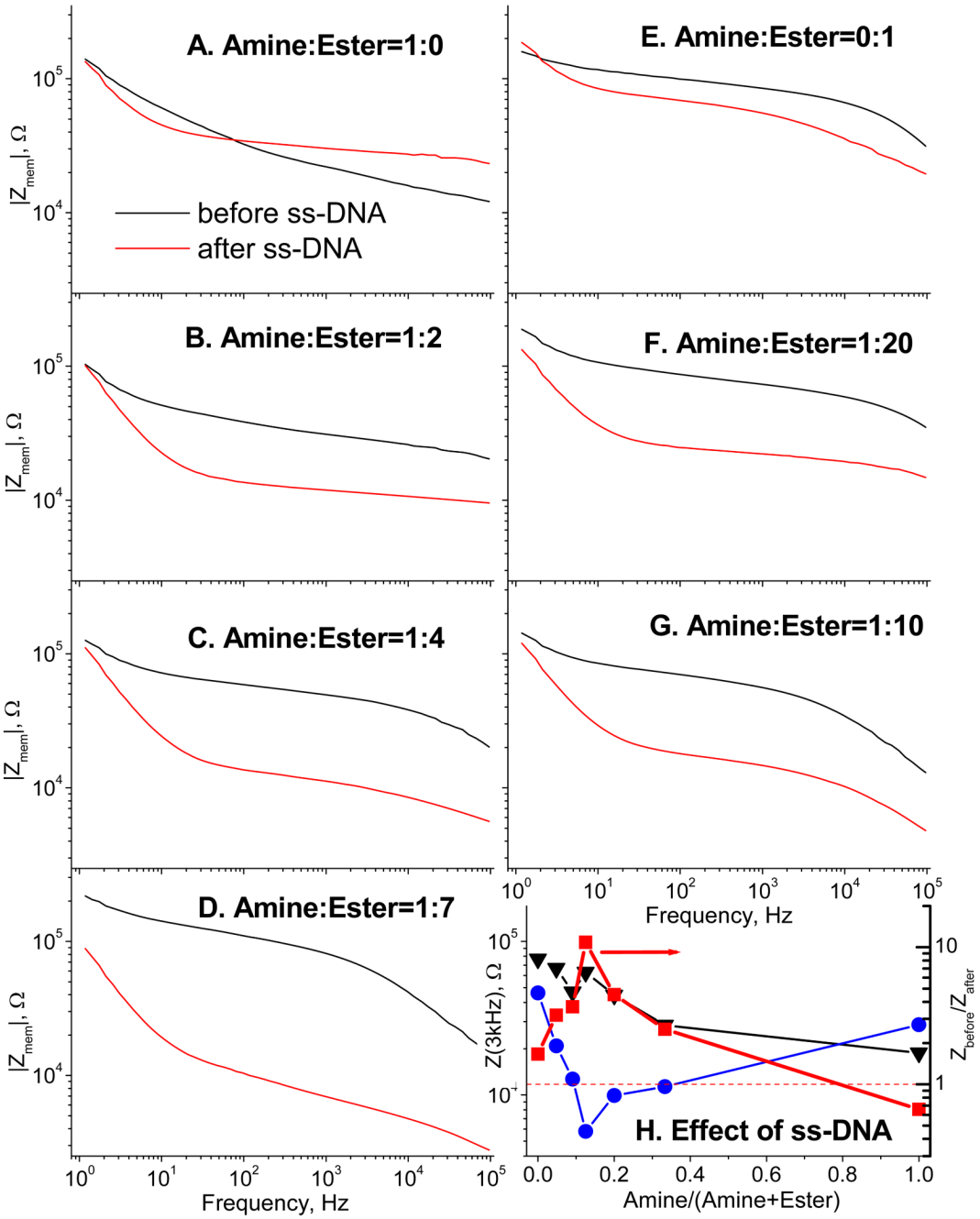

Figure 4.

Bode plots for ionic conductance (at 10 μM of KCl) through the membranes before (black) and after (red) immobilization of ss-DNA (16-mer). Different relative concentrations of the amine and ester (**A** – **G**) result in different surface densities of DNA. The effect of DNA binding, shown in H, as the ratio (red squares) of the impedance at 3 kHz before (black triangles) and after DNA binding (blue circles), has the optimal amine/ester ratio for maximal effect near amine:ester = 1:7, as in **D**. Note that for the surface with maximum amount of amines, the impedance increases after DNA binding.

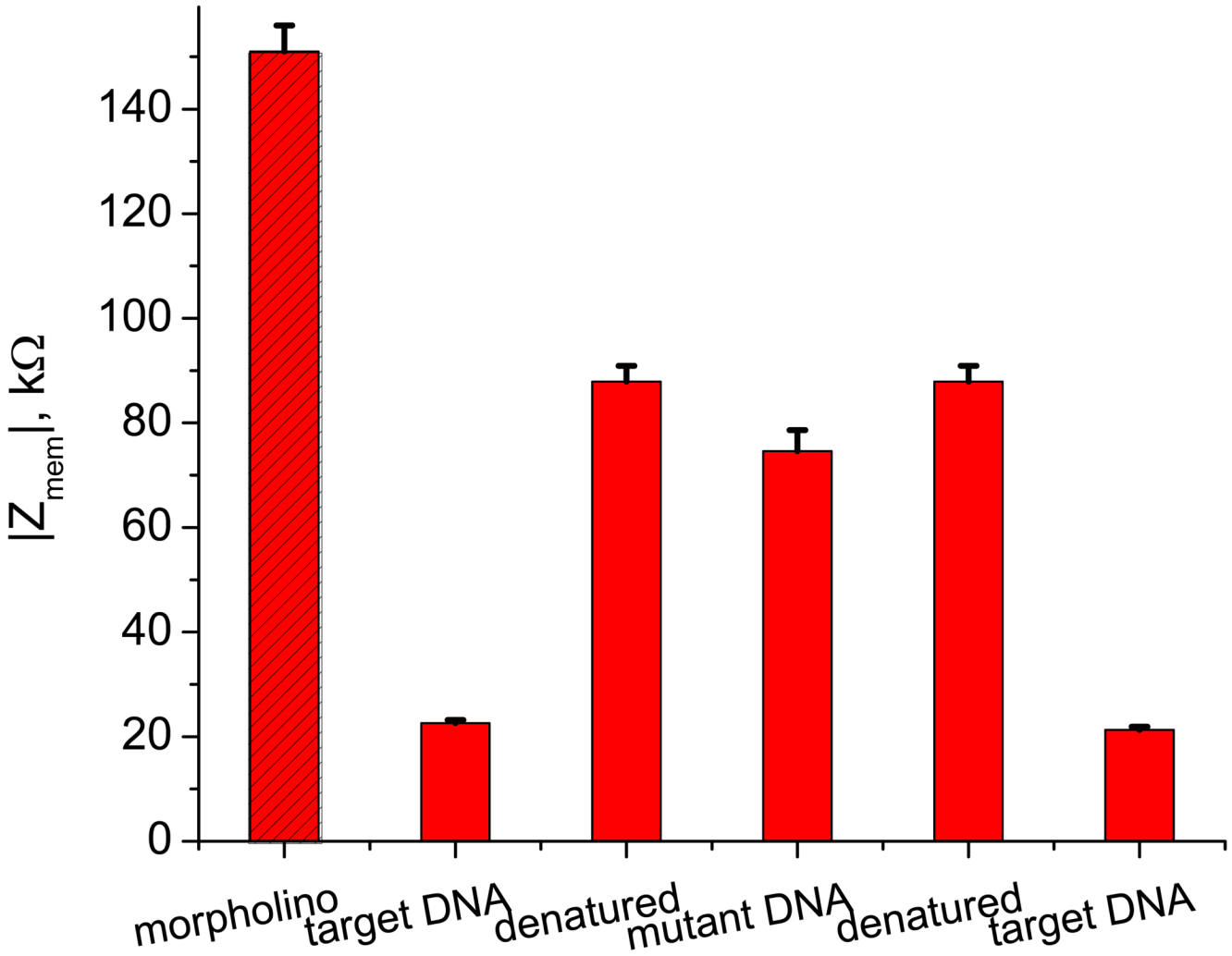

Figure 5.
The ionic impedance at 3 kHz through the morpholino modified membrane prepared with the 1:7 ratio of amine:ester silanes. Different stages of DNA sensing are shown, where target and mutant are the complementary and noncomplementary 15-mer DNA oligomers, respectively. The measurements were performed in 10 μM KCl buffer and denaturing was achieved with 9.0 M urea.

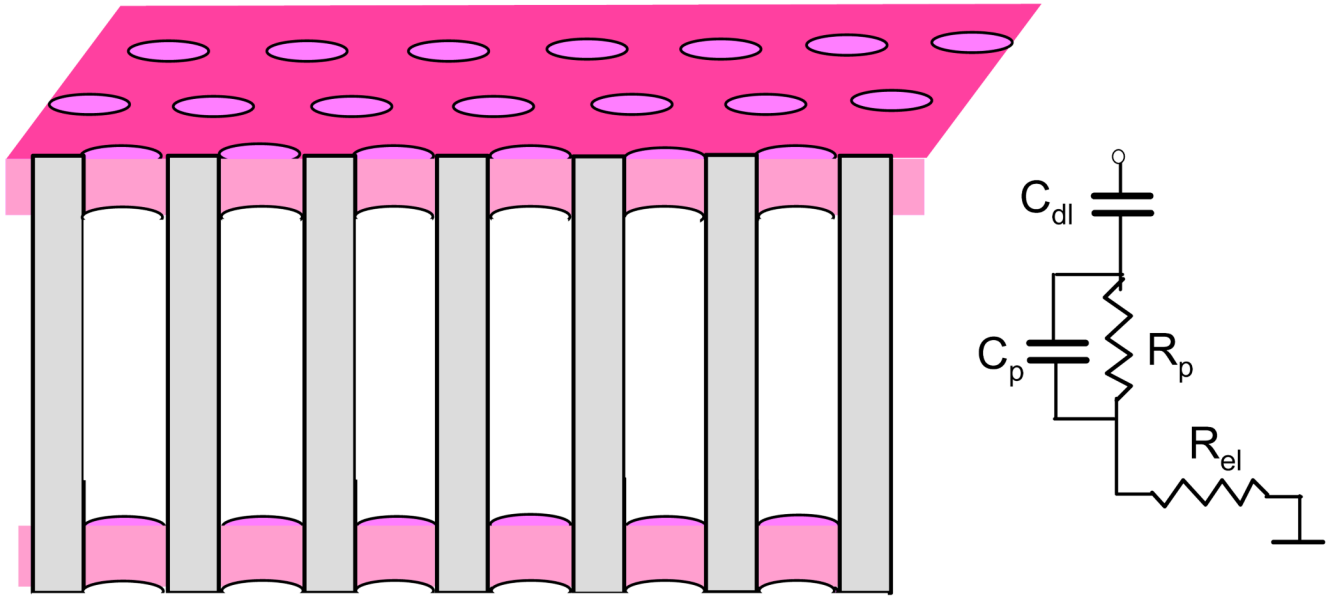

Scheme 1.